ISSN 1990-3413, Astrophysical Bulletin, 2020, Vol. 75, No. 4, pp. 376–383. © Pleiades Publishing, Ltd., 2020.
Russian Text © The Author(s), 2020, published in Astrofizicheskii Byulleten', 2020, Vol. 75, No. 4, pp. 424–432.

Quenched Galaxies in Clusters of Galaxies and Their Outskirts

F. G. Kopylova[a], * and A. I. Kopylov[a]

[a]*Special Astrophysical Observatory, Russian Academy of Sciences, Nizhnii Arkhyz, 369167 Russia*

**e-mail: flera@sao.ru*

Received March 27, 2020; revised September 18, 2020; accepted September 18, 2020

Abstract—Based on the SDSS catalog data the properties of galaxies with quenched star formation (QGs) within the "splashback"-radius of galaxy clusters R_{sp} and beyond it have been studied. We used a sample of 40 groups and galaxy clusters and a sample of field galaxies at $0.02 < z < 0.045$. The radii R_{sp} were defined from the observed integral distribution of the number of galaxies as a function of the squared distance from the center of the galaxy systems. We show that in galaxy clusters 72% of the QGs we have found are within R_{sp}. About 40% of these galaxies are late type ones with $fracDeV < 0.8$. Approximately 80% of galaxies with quenched star formation have stellar masses in the range of $\log M_*/M_\odot = [10; 11]$. We found that QGs of late types and of early types in a less degree have maximum angular radii $R_{90,r}$ and $R_{50,r}$ near the "splashback"-radius of groups and clusters of galaxies. Our results confirm the assumption that in the filaments directed toward clusters the quenched galaxies are more massive near the boundaries of the clusters of galaxies than at their ourskirts.

Keywords: galaxies: clusters, galaxies: star formation, galaxies: evolution

DOI: 10.1134/S1990341320040124

INTRODUCTION

Galaxy clusters, the largest gravitationally bound objects, increase their mass by accreting both dark matter and luminous one (groups of galaxies and galaxies) along filaments from the surrounding space (see, e.g., paper of Colberg et al., 1999). They demonstrate a wide range of spatial densities of galaxies: high-density areas in the center and low-density, almost field, on the periphery. Exploring galaxies in different environments, one can find out its role in quenching (reducing) star formation (SF) in galaxies (Balogh et al., 2004; Blanton and Moustakas, 2009; Peng et al., 2010). At the same time, it is possible to study the physical mechanisms operating in clusters, which cause the SF decrease and are responsible for the transformation of the galaxies (see, for example, paper of Boselli and Gavazzi, 2006). In the inner environment of galaxy clusters, there are various mechanisms leading to the decrease of the gas amount in galaxies and eventually to the decrease of star formation. These are tidal interactions between galaxies or between galaxies and a potential cluster well; collisions of galaxies at high velocities (galaxy harassment); stripping of gas as a result of frontal pressure (ram pressure stripping) of the intergalactic environment; thermal evaporation. According to observational data and results of modeling the main mechanism that leads to gas reduction in galaxies of clusters is ram pressure stripping (see, for example, paper of Lotz et al., 2019). Observational data (SDSS) show that stripping of gas in a spiral galaxy when it merges with a cluster is a slow process (van der Wel et al., 2010; von der Linden et al., 2010). For 2–4 Gyr (Wetzel et al., 2014) after the galaxy hits the cluster the SF rate practically does not change, then it quickly fades. It is found that SF quenching occurs effectively in galaxies of stellar masses $M_* = 10^9–10^{11.5} M_\odot$, that is, almost in each cluster galaxy with mass greater than $10^{13} M_\odot$ (Oman and Hudson, 2016) (SDSS data + modeling). It is also considered that SF should decrease to zero at the first passage of the galaxy through the center of the cluster. Observations show that the SF rate in star-forming galaxies continously decreases from the periphery to the center of galaxy clusters (see, for example, papers of Paccagnella et al., 2016; von der Linden et al., 2010), and in galaxy clusters it is lower than in the field (see, for example, Gavazzi et al., 2006; Haines et al., 2013). Studies of the SF rate in the clusters' outskirts showed that galaxies with quenched star formation are observed even beyond the virial radii of clusters. According to SDSS and model calculations about of 40% of galaxies near massive systems are escaped galaxies with quenched SF, and their orbits can reach about $2.5R_{200m}$ (Wetzel et al., 2012), where R_{200m} is the radius of the sphere, inside which the system density is 200 times the mean density of the Universe. It is also defined that some of galaxies could lose gas within low-mass groups falling into the galaxy cluster (see, for example, Balogh et al., 2000).

In galaxy clusters (SDSS data) there is a significant number of spirals among the galaxies with quenched SF (van der Wel et al., 2010). Hamabata et al. (2019)

(SDSS data and model calculations) found the radius of galaxy cluster ($r \sim 0.6h^{-1}$ Mpc), that bounds the area inside which red-spiral galaxies with SF quenching appear. In galaxy clusters of the Local universe (WINGS galaxy sample) there are also transition types—from star-forming galaxies to passive ones (Paccagnella et al., 2016). They are found within $0.6R_{200}$ and are rare in the field. When considering clusters as laboratories, where galaxy transformations occur Cebrian and Trujillo (2014); Poggianti et al. (2013) showed that early-type galaxies in clusters are smaller in size than field galaxies.

To determine how the system properties of galaxies with quenched star formation change along the normalized radius (up to $3R/R_{200}$), in our study we used a sample of 40 galaxy clusters (Kopylova and Kopylov, 2018, 2019). It consists of clusters of galaxies with registered X-ray emission, which are located in the Leo and Hercules supercluster regions. Additionally, we include close systems: the clusters A1367, A1656, and 8 galaxy groups from Kopylova and Kopylov (2015). Selecting systems in the local Universe ($0.02 < z < 0.045$) we aimed to cover the maximum range of radial velocity dispersion—from 300 km s^{-1} to 950 km s^{-1}. For the study we selected galaxies brighter than $M_K = -21.5^{\mathrm{m}}$ which corresponds to approximately $M_r = -18.3^{\mathrm{m}}$.

In this work, we used data of the SDSS (Sloan Digital Sky Survey Data Release 10) (Ahn et al., 2014) and 2MASS XSC (2MASX, Two-Micron ALL-Sky Survey Extended Source Catalog (Jarrett et al., 2000)) catalogs, and NED (NASA Extragalactic Database).

The paper is organized as follows. The second section describes the sample of galaxies with quenched SF, the outskirts of galaxy clusters is shown in units of radius R_{200}. In the third section, we consider the characteristics of QGs: galaxy distributions by absolute magnitude, by the parameter that characterizes the de Vaucouleur profile contribution into the surface brightness profile, by the parameter equal to the axis ratio of galaxies. The change of radii limiting 90% and 50% of Petrosian flux in the r-band ($R_{90,r}$, $R_{50,r}$), early- and late-type galaxies along the normalized cluster radius galaxies up to $3R/R_{200}$ has been studied. In Conclusion the main results are listed. We took the following values of cosmological parameters: $\Omega_m = 0.3$, $\Omega_\Lambda = 0.7$, $H_0 = 70$ km s^{-1} Mpc^{-1}.

SAMPLE OF GALAXIES WITH QUENCHED STAR FORMATION

The specific star formation rate ($sSFR$) in a galaxy is defined as the integrated star formation rate divided by the stellar mass, $sSFR = SFR/M_*$. In the distribution of galaxies by the specific star formation rate ($\log sSFR$) the minimum is usually found, which separates the galaxies actively forming stars (active galaxies) from galaxies that have quenched star formation (quenched galaxies—QGs) and galaxies without SF (passive). Using data on sSFR and galaxy stellar mass from the SDSSDR10 catalog, in our papers (Kopylova and Kopylov, 2018, 2019) we selected QGs and passive galaxies, following the condition $\log s\mathrm{SFR} < -10.75$ [yr^{-1}]. Distribution of galaxies by specific star formation rate ($\log s$SFR) has a long tail extending into the area of galaxies without SF. In this paper, we omit galaxies of this type ($\log s\mathrm{SFR} < -12$ [yr^{-1}] (Oemler et al., 2017)), and consider only QGs, i.e., galaxies with $-12 < \log s\mathrm{SFR} < -10.75$ [yr^{-1}]. Groups and clusters of galaxies in our sample— have radial velocity dispersions σ in the range of 300–950 km s^{-1} (which corresponds to masses $M_{200} = (0.5 - 14.7) \times 10^{14}\, M_\odot$). We divided the entire interval into σ bins, with subsamples of N objects (shown in Fig. 2–Fig. 4 by lines of different types and colors):

$$800\text{–}950 \text{ km s}^{-1} \text{ or } (9\text{–}14.5)\times10^{14} M_\odot, \quad N = 2;$$

$$600\text{–}800 \text{ km s}^{-1} \text{ or } (4\text{–}9)\times10^{14} M_\odot, \quad N = 6;$$

$$500\text{–}600 \text{ km s}^{-1} \text{ or } (2\text{–}4)\times10^{14} M_\odot, \quad N = 7;$$

$$400\text{–}500 \text{ km s}^{-1} \text{ or } (1\text{–}2)\times10^{14} M_\odot, \quad N = 11;$$

$$300\text{–}400 \text{ km s}^{-1} \text{ or } (0.5\text{–}1)\times10^{14} M_\odot, \quad N = 14.$$

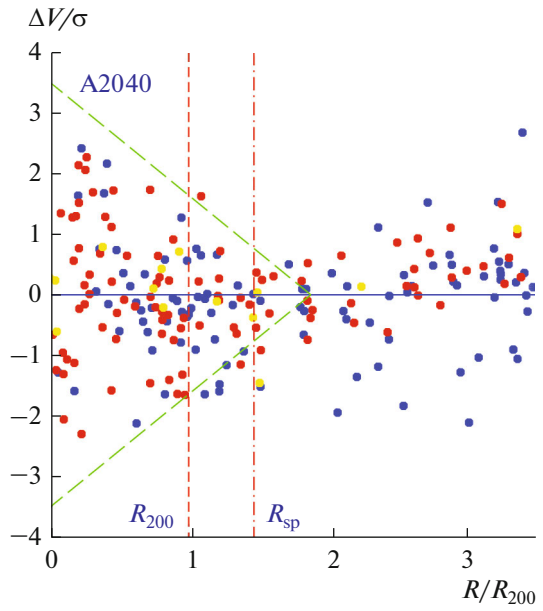

Fig. 1. Phase-space diagram: velocity as a function of radius. The velocity is ratio of the difference between the radial velocities of galaxies and the mean radial velocity of the cluster to the dispersion radial velocity dispersion. The R/R_{200} radii are galaxy distances from the center, normalized by the radius R_{200}. Red circles show galaxies with quenched SF ($-12.0 < \log s\mathrm{SFR} < -10.75$ [yr^{-1}]), yellow—"passive" ones ($\log sSFR < -12$ [yr^{-1}]). Green model lines (Barsanti et al. (2018)) separate a cluster area with virialized members.

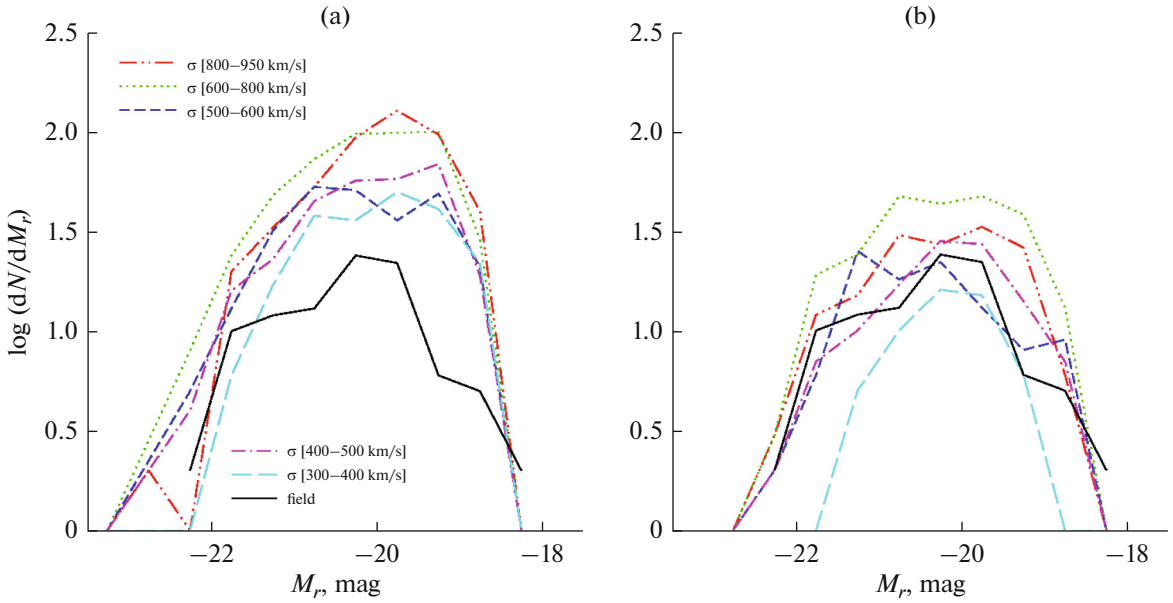

Fig. 2. Distributions of QGs by absolute value M_r ($M_r < -18.3^m$): (a) within the normalized radius R_{sp} and (b) beyond it ($R_{sp}/R_{200} < R/R_{200} < 3R/R_{200}$). Groups and clusters of galaxies are binned in accordance with the radial velocity dispersion σ and are shown by different lines. The solid black line shows the distribution of galaxies in the field.

For some of the sample objects (mostly, early-type galaxies located within the radius of R_{200}) there were no data on *sSFR* in DR10 and we estimated *sSFR* by the $u-r$ and $g-r$ colors of the galaxies, their absolute magnitudes and by the *fracDeV* parameter based on available measurements of other galaxies. In order to compare the results of our study we also selected two fields, practically free from galaxy clusters. They are located between the Hercules and Leo superclusters. The first one has the center coordinates (14.5^h, 35°), the radius 300 arcminutes, the redshift range $0.030 < z < 0.045$ ($N = 219$), for the second field, with the same redshifts and radius, the center coordinates are (13.5^h, 5°) ($N = 147$) (Kopylova and Kopylov, 2018). To improve the statistics of measurements we consider both fields together.

We constructed and analyzed phase-space diagrams for all objects in the sample. One of the diagrams, for the galaxy cluster A2040, is shown in Fig. 1 as an example. The radius R_{200}[1], defined from the dispersion of the radial velocities of galaxies, and the radius R_{sp}, which we determined from the observed cluster profile (integral distribution of the number of galaxies depending on the squared distances from the cluster center (Kopylova and Kopylov, 2018, 2019)) are marked. The radius R_{sp} (previously denoted as R_h and described in detail in Kopylova and Kopylov (2016)), is identified with the "splashback"-radius and represents the cluster boundary, the place of location of the orbit apocenters of the galaxies that are flung out after the first visit to the center, i.e., the galaxies that are already gravitationally bound to the cluster. By estimates of Wetzel et al. (2012) the escaped galaxies can represent up to 40% of all galaxies in the region between R_{sp} and R_{200}. Green lines (by the model of Barsanti et al. (2018)) in Fig. 1 roughly separate the virialized part of the galaxy cluster. Galaxies outside these lines are presumably falling into the cluster for the first time. For other galaxy clusters, the results of the R_{sp} measurements are given in Kopylova and Kopylov (2018, 2019). In the figures of these papers we showed that the proportion of galaxies with quenched star formation, QGs, decreases with increasing galaxy cluster radii, and approaches the field values at $3R/R_{200}$.

[1] The radius, within which the system density is 200 times the critical density of the Universe.

PROPERTIES OF GALAXIES WITH QUENCHED STAR FORMATION

3.1. Distributions of QGs by Absolute Magnitude, by Contribution of the de Vaucouleur Profile to the Surface Brightness Profile, and by the Axes Ratio

In 40 galaxy clusters and their surroundings we found 2368 galaxies with quenched star formation ($R/R_{200} < 3R/R_{200}$, $M_r < -18.3^m$). Nearly 72% of them are located in the inner parts of clusters, within the normalized radius R_{sp}. QGs of later types, classified by parameter *fracDeV* ≤ 0.8, amount to 40%, the rest galaxies are of types E, SO, Sa, and SBa. Among the selected 2368 QGs 80% are galaxies with stellar masses

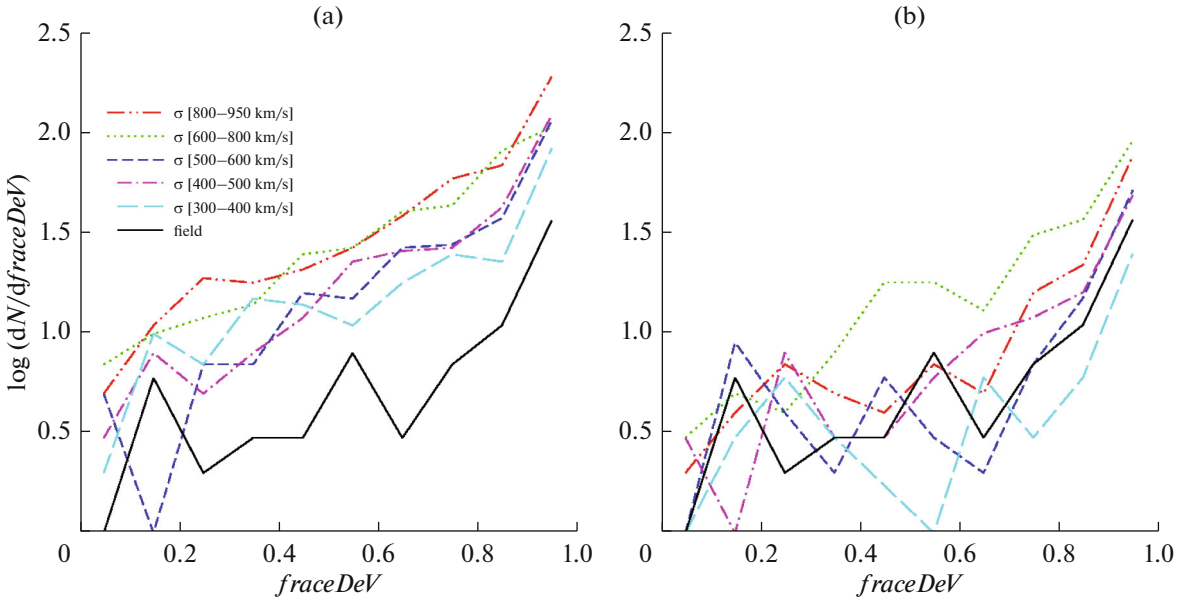

Fig. 3. The same as in Fig. 2, but by the parameter *fracDeV* (SDSS), describing the contribution of the de Vaucouleur profile to the galaxy surface brightness.

in the range of $\log M_*/M_\odot = [10, 11]$, with the average value $\log M_*/M_\odot = 10.48 \pm 0.01$. This corresponds to the data of model calculations performed by Contini et al. (2020).

The distributions of QGs by absolute magnitudes within the normalized radius R_{sp} and beyond it are demonstrated in Figs. 2a and 2b. The errors of distributions are small (less than 0.1, but for end points), they are estimated as $\sqrt{dN}$, where dN is the number of galaxies in the range dM_r. It can be noted that in clusters ($R < R_{sp}$) the galaxies under investigation are brighter (the distribution has a tail towards the bright ones) than in the field (black line) in all bins except one, which corresponds to groups of galaxies with $\sigma = 300–400$ km s^{-1} (blue line). Outside R_{sp} the same groups show the absolute magnitude variations in a smaller range than galaxies in clusters and the field ones. The average value of the absolute magnitude of the QGs sample within R_{sp} is $\langle M_r \rangle = -20.09 \pm 0.02$. Outside of R_{sp} and in the field QGs are brighter: $\langle M_r \rangle = -20.27 \pm 0.03$ and $\langle M_r \rangle = -20.35 \pm 0.09$, respectively.

Figures 3a and 3b show distributions of galaxies by the parameter *fracDeV*, which characterizes the contribution of the de Vaucouleur profile to the surface brightness profile. Note that there is no dedicated range of radial velocity dispersions σ. In each bin there are spiral galaxies with *fracDeV* < 0.4, both within R_{sp} and beyond it, as well as in the field. Number of QGs of early types with *fracDeV* ≥ 0.8 within R_{sp} and beyond it are by 25 and 38% higher than the number of spiral galaxies. The number of galaxies of these types in the field is approximately the same.

The distribution of the axes ratio b/a for the observed surface brightness profiles of QGs within and beyond the radius of R_{sp} is shown in Figs. 4a and 4b. It can be noted that QGs have a variety of axes ratios—from 0.25 to 1.00. On average the ratio b/a is equal to 0.6 ± 0.01 for all studied regions, and the number of galaxies with b/a values greater or less than this threshold is approximately the same in the field and in the vicinity of galaxy clusters. But in galaxy clusters, within R_{sp}, the galaxies with $b/a > 0.6$ represent more than 14%. Besides, in Fig. 4 one can see that spiral galaxies with $b/a < 0.4$ are particularly distinguished.

By all parameters we can make an overall conclusion that in the vicinity of the lowest-mass galaxy groups those with quenched SF are less in number, even in comparison with the field (in Figs. 2, 3b, 4b the blue lines are located below the others).

3.2. The Change of QGs Sizes along the Radius of Galaxy Clusters

In order to study how sizes of galaxies change, the comparison of Petrosian radii can be used as a method that is independent of galaxy distances. The SDSS catalog provides the data on R_{50} and R_{90}, the angular Petrosian radii in all SDSS-bands, containing 50% and 90% of a Petrosian flux. The Petrosian flux in any band is measured as the flux within $2R_P$, where R_P is the angular radius inside which the ratio of the local surface brightness at a radius r from the center of an object to the mean surface brightness within r is equal

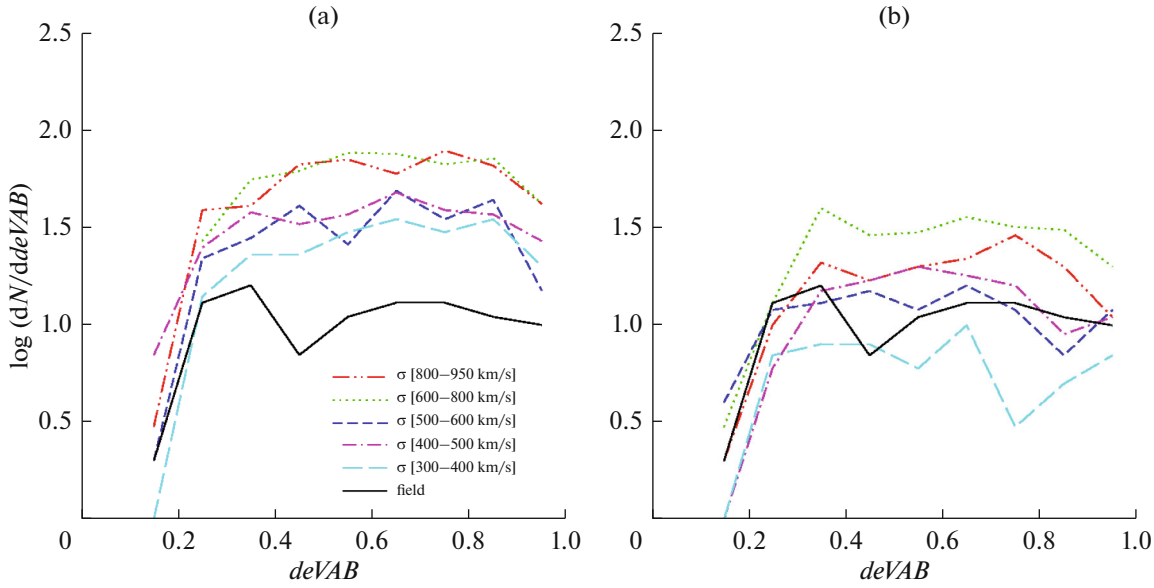

Fig. 4. The same as in Fig. 2, but by the parameter *DeV AB*, that characterizes the galaxy axes ratio.

to 0.2. We used measurements in the *r*-filter. According to Raichoor and Andreon (2014), the quenching rate of star formation in clusters with masses of $\log M_{200}/M_{\odot} > 14$ (as in our sample) does not depend on the mass, richness, and iron abundance in the cluster. In our paper (Kopylova and Kopylov, 2019) (Fig. 7) we have shown that the change in the fractions of galaxies with quenched SF at a fixed stellar mass is the same in all mass ranges considered, except for the bin for galaxy clusters with $\log M_*/M_{\odot} = [11; 11.5]$ and $\sigma = 300{-}400$ km s^{-1}. In such systems there are practically no massive galaxies with quenched SF outside of the virial radius. Thus, to investigate the size distribution of galaxies along the radius, normalized by R_{200}, we stacked data for all the systems.

We divided the QGs sample into two subsamples: the early-type galaxies with *fracDeV* ≥ 0.8 and the later-type ones with *fracDeV* < 0.8. The panels in Fig. 5 show changes in the average Petrosian radius $R_{90,r}$ along the normalized radius of galaxy clusters for both of them. Similar values of the Petrosian radius for the field galaxies are given for comparison, along with the average radius of all galaxies in the sample $\langle R_{sp} \rangle = (1.54 \pm 0.06)\, R_{200}$ (a solid vertical line) and the ranges of its variation $R_{sp} = [1.9; 1.2]$ (Kopylova and Kopylov, 2018, 2019).

There are 58% of early-type galaxies in the sample. The galaxies with stellar masses in the range $\log M_* = [10, 11]$ represent 83% among them and 74% in the subsample of late-type galaxies. Figures 5c and 5d show changes in the angular radii $R_{90,r}$ for these galaxies. Radii of late-type galaxies with stellar masses in the ranges $\log M_* = [10; 10.5]$ and $\log M_* = [10.5; 11.0]$ near R_{sp} are about 20 and 13% larger than in the central regions. For early-type galaxies in the same stellar mass ranges the radii change is about 11%. We found that such an increase in angular radii for galaxies near R_{sp} is also observed for $R_{50,r}$, but to a less degree, by 13 and 11%, respectively. Beyond R_{sp} for galaxy clusters, the angular radii of galaxies $R_{90,r}$ decrease to the values that are close to the field ones. In the area between R_{200} and R_{sp} different galaxies are observed (Fig. 1). Some of them flew out of the cluster, and the others, moving in the opposite direction, just come up to it. Since the galaxy sizes in this boundary area are larger than in the central regions of clusters, then we can assume that here, basically, there are galaxies that are not ejected from the system, but falling on it.

The low-mass late-type galaxies in the mass range $\log M_* = [9.5; 10.0]$ (presented in blue in Fig. 5b) show no radius changes as well, while the early-type galaxies (red), on the contrary, grow in size by approximately 30% to the center of galaxy clusters compared to the periphery. Their sizes are bigger than those of the field galaxies, although the data accuracy for the field estimates is rather poor—there are few galaxies in the sample. The most massive galaxies in the range $\log M_* = [11.0; 11.5]$ (Fig. 5e) also do not show significant changes in size, although they are still smaller than field galaxies, especially the late-type ones. In Fig. 5a, where all studied galaxies are presented without fixing the stellar mass, changes in the radius $R_{90,r}$ of the late-type galaxies are shown—the galaxy radii increase by 25% to $3R/R_{200}$ and become of the same value as in the field. At the same time, the early-type galaxies, which are located in the inner parts of clusters, practically do not differ from the field galaxies, but at $3R/R_{200}$ we observe an increase in their size by 12%.

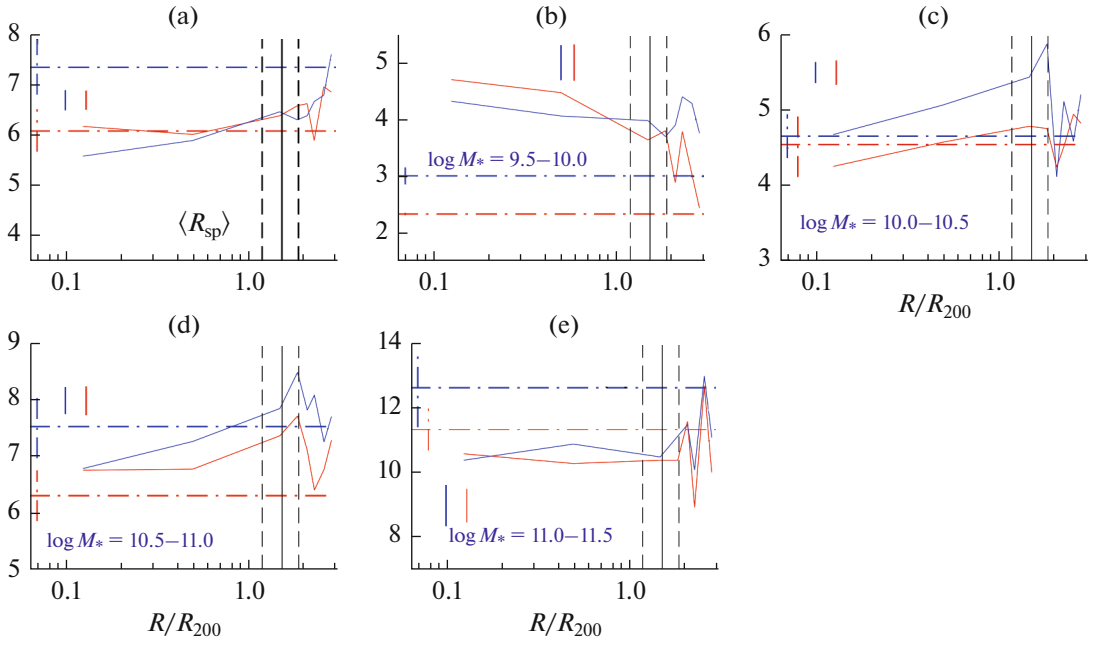

Fig. 5. Petrosian radius R_{90} in kpc in the filter r depending on the normalized radius R/R_{200} for the studied galaxies in total (a) and binned by stellar masses (b)–(e). Data for galaxy clusters are stacked taking account of their normalized radii. QGs-galaxies of early types, defined by the parameter $fracDeV \geq 0.8$ and the late-type ones with $fracDeV < 0.8$ are shown with red and blue solid lines,respectively. Short red and blue lines correspond to the average errors of the radius measurements. Solid and dashed vertical lines show the mean R_{sp} and the range of its changes. Dashed horizontal lines correspond to the average values of R_{90} for the field, the vertical ones—to the error bars.

According to, for example, Rhee et al. (2020), in the inner environment of galaxy clusters the lowmass spiral galaxies on $z = 0.8$ with $\log M_*/M_\odot = [9, 10]$ can better resist the direct gas stripping process. Perhaps, these galaxies have more central gas. As a result, their star formation is not completely quenched and still continues for a long time after they entered the cluster, leading to their weight and size growth.

As for massive galaxies, they have a smaller gas fraction and lose it faster and earlier, before the cluster entering (Rhee et al., 2020) within the filaments. Other studies of a sample of 700 galaxies ($z < 0.063$, SDSS data) show that the size of spiral galaxies in clusters is 15% smaller, than in the field. Poggianti et al. (2013) found that the early-type galaxies in clusters are also smaller in size compared to the field ones.

SUMMARY AND CONCLUSIONS

Quenching of star formation in galaxy clusters and their outskirts is a consequence of the gas loss in haloes, disks, and inner areas of galaxies. As a result, the galaxy does not have enough "fuel" to form stars. In this case, both processes play an important role: effects within galaxies clusters and those ones, which act in groups of smaller masses and in filaments stretching to galaxy clusters. Several papers have been devoted to studying the properties of galaxies in filaments. Using the GAMA survey, Alpaslan et al. (2016) obtained that isolated spiral galaxies have higher stellar masses and lower values of the SF rate in the central regions of filaments than at their periphery. The SDSS data allowed Chen et al. (2017) to conclude that galaxies in filaments are more massive than outside of them despite the local density of the same value. Study of SF quenching in the vicinity of 14 clusters the WINGS galaxy survey showed that this process is the most effective in the direction of filaments (Salerno et al. 2020). In Santiago Bautista et al. (2020) it is also shown that in the filaments the galaxies are more massive and the SF rate in them is lower than in the surrounding field. It is concluded, that it is likely that the galaxies here are experienced merging, i.e. filaments significantly influence galaxy evolution. According to our studies of late-type QGs, near R_{sp} the galaxies with the maximum angular radius of $R_{90,r}$ probably have already lost their gas being a part of low-mass groups falling onto a cluster along filaments.

The star formation rate in galaxies decreases with local density increasing In galaxy clusters this corresponds to a decrease in the distance from the center (Balogh et al., 2004). There are several models of SF quenching in galaxy clusters. In the "rapid quenching" model the SF is quenched for a short time (less than 1 Gyr) after the galaxy has entered the cluster, (see, for example, papers Balogh et al., 2000). Taranu

et al. (2014); von der Linden et al. (2010) considered models of slow SF quenching. The model, best describing SF quenching in galaxies, is the "delayed-then-rapid" one. In the framework of this model the galaxy after entering a cluster has its SF unchanged for several Gyrs, and then SF quickly quenched (Foltz et al., 2018; Fossati et al., 2017; Wetzel et al., 2013).

In a sample of 40 galaxy clusters ($0.02 < z < 0.045$) located mainly in the Leo, Hercules, and Coma superclusters we selected galaxies with quenched star formation ($-12.0 < \log sSFR < -10.75$ [yr^{-1}]). To learn how properties of QGs change with their distance from the cluster center, we determined the observed "splashback"-radius. It shows the cluster halo boundary, i.e. area of location of both the galaxies, that flung out after the first system passage, and those approaching the system for the first time along with filaments. The main part of QGs in the sample (of about 80%) is within the radius R_{sp}, their absolute magnitudes being $M_r = -20.09^m \pm 0.02$. If QGs are binned by stellar mass, then 80% of galaxies have stellar masses in the interval $\log M_*/M_\odot = [10, 11]$ with the mean value $\log M_*/M_\odot = 10.48 \pm 0.01$. The QGs sample has also the following mean values of parameters according to SDSS data: $\langle fracDeV \rangle = 0.76 \pm 0.01$ and $\langle DeVAB \rangle = 0.61 \pm 0.01$. Among the galaxies with quenched SF, about 40% are the late-type ones located within R_{sp}. There are 63% of late-type galaxies with an axis ratio of $b/a < 0.6$ within R_{sp} and 72%—beyond it.

Radii of late-type galaxies in the stellar mass range $\log M_* = [10; 10.5]$ and $\log M_* = [10.5; 11.0]$ are by approximately 20 and 13% larger near the radius R_{sp} than in the central areas. Radii of early-type galaxies for the same stellar mass ranges have changed by about 11%. Beyond "splashback"-radius of galaxy clusters R_{sp} the angular radii $R_{90,r}$ of galaxies decrease to values close to the field ones. The main results of our work can be formulated as follows. Sizes of the main amount of QGs galaxies of late types (and early-type galaxies, to a lesser degree), their Petrosian angular radii $R_{90,r}$, $R_{50,r}$ are maximum near the boundary of galaxy clusters, defined by the "splashback"-radius R_{sp}.

ACKNOWLEDGMENTS

This research has made use of the NASA/IPAC Extragalactic Database (NED, http://nedwww.ipac.caltech.edu), which is operated by the Jet Propulsion Laboratory, California Institute of Technology, under contract with the National Aeronautics and Space Administration, Sloan Digital Sky Survey (SDSS, http://www.sdss.org), which is supported by Alfred P. Sloan Foundation, the participant institutes of the SDSS collaboration, National Science Foundation, and the United States Department of Energy and Two Micron All Sky Survey (2MASS, http://www.ipac.caltech.edu/2mass/releases/allsky/)

CONFLICT OF INTEREST

The authors declare no conflict of interest regarding this paper.

REFERENCES

1. C. P. Ahn, R. Alexandroff, C. Allende Prieto, et al., Astrophys. J. Suppl. **211** (2), 17 (2014).
2. M. Alpaslan, M. Grootes, P. M. Marcum, et al., Monthly Notices Royal Astron. Soc. **457** (3), 2287 (2016).
3. M. L. Balogh, I. K. Baldry, R. Nichol, et al., Astrophys. J. **615**, L101 (2004).
4. M. L. Balogh, J. F. Navarro, and S. L. Morris, Astrophys. J. **540**, 113 (2000).
5. S. Barsanti, M. S. Owers, S. Brough, et al., Astrophys. J. **857** (1), 71 (2018).
6. M. R. Blanton and J. Moustakas, Annual Rev. Astron. Astrophys. **47** (1), 159 (2009).
7. A. Boselli and G. Gavazzi, Publ. Astron. Soc. Pacific **118**, 517 (2006).
8. M. Cebrian and I. Trujillo, Monthly Notices Royal Astron. Soc. **444** (1), 682 (2014).
9. Y.-C. Chen, S. Ho, R. Mandelbaum, et al., Monthly Notices Royal Astron. Soc. **466** (2), 1880 (2017).
10. J. M. Colberg, S. D. M. White, A. Jenkins, and F. R. Pearce, Monthly Notices Royal Astron. Soc. **308** (3), 593 (1999).
11. E. Contini, Q. Gu, X. Ge, et al., Astrophys. J. **889** (2), 156 (2020).
12. R. Foltz, G. Wilson, A. Muzzin, et al., Astrophys. J. **866** (2), 136 (2018).
13. M. Fossati, D. J. Wilman, J. T. Mendel, et al., Astrophys. J. **835** (2), 153 (2017).
14. G. Gavazzi, A. Boselli, L. Cortese, et al., Astron. and Astrophys. **446** (3), 839 (2006).
15. C. P. Haines, M. J. Pereira, G. P. Smith, et al., Astrophys. J. **775** (2), 126 (2013).
16. A. Hamabata, T. Oogi, M. Oguri, et al., Monthly Notices Royal Astron. Soc. **488** (3), 4117 (2019).
17. T. H. Jarrett, T. Chester, R. Cutri, et al., Astron. J. **119**, 2498 (2000).
18. F. G. Kopylova and A. I. Kopylov, Astrophysical Bulletin **70** (2), 123 (2015).
19. F. G. Kopylova and A. I. Kopylov, Astrophysical Bulletin **71** (3), 257 (2016).
20. F. G. Kopylova and A. I. Kopylov, Astrophysical Bulletin **73** (3), 267 (2018).
21. F. G. Kopylova and A. I. Kopylov, Astrophysical Bulletin **74** (4), 365 (2019).
22. M. Lotz, R.-S. Remus, K. Dolag, et al., Monthly Notices Royal Astron. Soc. **488** (4), 5370 (2019).
23. A. Oemler, Jr., L. E. Abramson, M. D. Gladders, et al., Astrophys. J. **844** (1), 45 (2017).
24. K. A. Oman and M. J. Hudson, Monthly Notices Royal Astron. Soc. **463**, 3083 (2016).
25. A. Paccagnella, B. Vulcani, B. M. Poggianti, et al., Astrophys. J.**816**, L25 (2016).

26. Y.-J. Peng, S. J. Lilly, K. Kovac, et al., Astrophys. J. **721** (1), 193 (2010).

27. B. M. Poggianti, R. Calvi, D. Bindoni, et al., IAU Symp. **295**, pp. 151–154 (2013).

28. A. Raichoor and S. Andreon, Astron. and Astrophys. **570**, A123 (2014).

29. J. Rhee, R. Smith, H. Choi, et al., Astrophys. J. Suppl. **247** (2), 45 (2020).

30. J. M. Salerno, H. J. Martínez, H. Muriel, et al., Monthly Notices Royal Astron. Soc. **493** (4), 4950 (2020).

31. I. Santiago-Bautista, C. A. Caretta, H. Bravo-Alfaro, et al., Astron. and Astrophys. **637**, A31 (2020).

32. D. S. Taranu, M. J. Hudson, M. L. Balogh, et al., Monthly Notices Royal Astron. Soc. **440** (3), 1934 (2014).

33. A. van der Wel, E. F. Bell, B. P. Holden, et al., Astrophys. J. **714** (2), 1779 (2010).

34. A. von der Linden, V. Wild, G. Kauffmann, et al., Monthly Notices Royal Astron. Soc. **404** (3), 1231 (2010).

35. A. R. Wetzel, J. L. Tinker, and C. Conroy, Monthly Notices Royal Astron. Soc. **424**, 232 (2012).

36. A. R. Wetzel, J. L. Tinker, C. Conroy, and F. C. van den Bosch, Monthly Notices Royal Astron. Soc. **432** (1), 336 (2013).

37. A. R. Wetzel, J. L. Tinker, C. Conroy, and F. C. van den Bosch, Monthly Notices Royal Astron. Soc. **439**, 2687 (2014).